

Recycling Parrondo games

This article has been downloaded from IOPscience. Please scroll down to see the full text article.

2006 J. Phys. A: Math. Gen. 39 1285

(<http://iopscience.iop.org/0305-4470/39/6/005>)

View [the table of contents for this issue](#), or go to the [journal homepage](#) for more

Download details:

IP Address: 171.66.16.108

The article was downloaded on 03/06/2010 at 04:59

Please note that [terms and conditions apply](#).

Recycling Parrondo games

Roberto Artuso^{1,3}, Lucia Cavallasca¹ and Giampaolo Cristadoro²

¹ Center for Nonlinear and Complex Systems and Dipartimento di Fisica e Matematica, Università dell'Insubria, Via Valleggio 11, 22100 Como, Italy

² Max Planck Institute for the Physics of Complex Systems, Nöthnitzer Str 38, D-01187 Dresden, Germany

Received 25 October 2005, in final form 13 December 2005

Published 25 January 2006

Online at stacks.iop.org/JPhysA/39/1285

Abstract

We consider a deterministic realization of Parrondo games, and use periodic orbit theory to analyse their asymptotic behaviour.

PACS number: 05.45.–a

(Some figures in this article are in colour only in the electronic version)

1. Introduction

Directed transport has received remarkable attention for a number of years now, since it has been recognized as a crucial issue in a number of physical and biological contexts (see the review [1] and references therein). A striking phenomenon in this context is *ratchets* behaviour, where currents may flow in a counter intuitive direction. Parrondo games (see [2] and references therein) offer a remarkable and simple illustration of these subtle transport properties: a random combination of two losing games may result in a winning strategy. In this paper, we present a deterministic analogue of Parrondo games, in the form of a (piecewise linear), periodic map on the real line, and study transport properties by means of periodic orbit expansions [3]: in this simple setting they allow us to perform analytic evaluations of the relevant quantities, while providing a highly effective perturbative technique to get accurate estimates in more general cases (for instance by considering nonlinear mappings). The paper is organized as follows: in section 2 we construct a deterministic realization of Parrondo games in the form of a one-dimensional mapping on the real line, in section 3 we briefly review how to study transport properties of deterministic systems by periodic orbits expansions, in section 4 we apply such a theory to Parrondo mappings and discuss some features of our findings, and in section 5 we give our conclusions, and possible future developments of the present work.

³ Also at Istituto Nazionale Fisica Nucleare, Sezione di Milano, Via Celoria 16, 20133 Milano, Italy, and CNR-INFN, Sezione di Como.

2. One-dimensional Parrondo mappings

Let us briefly recall the simplest implementation of Parrondo games: we start from two simple games \mathcal{A} and \mathcal{B} : \mathcal{A} is a simple-coin tossing game with winning probability p and losing probability $(1 - p)$: each time the game is played the player toss the coin: if he/she wins then the capital (an integer value, which we denote by X) is increased by one unit, otherwise it is decreased by the same amount. Game \mathcal{B} is a little bit more complicated, as it requires two ‘coins’, selected upon inspection of the present value of the capital: if $X = 0_{\text{mod } M}$ winning/losing probability is $p_1/1 - p_1$, while in the opposite case ($X \neq 0_{\text{mod } M}$) the winning/losing probability is $p_2/1 - p_2$: where M is a fixed integer. Now suppose that at any integer time step n (starting from zero) a game is played: $X(n)$ which represents the instantaneous value of the capital. It turns out that fine tuning of the parameters leads to a paradoxical behaviour: namely take $M = 3$, $p = 1/2 - \epsilon$, $p_1 = 1/10 - \epsilon$, $p_2 = 3/4 - \epsilon$, for a sufficiently small value of ϵ : both games are in this case slightly unfair: if the player keeps on playing \mathcal{A} or \mathcal{B} the capital will drop down linearly, while playing \mathcal{A} or \mathcal{B} in random order (for instance with probability $1/2$) results in a winning strategy, where on the average the capital increases linearly with time! The paradox can be explained by a Markov chain analysis [4].

We now map the problem to a dynamical setting: that is we want to introduce a map F_p on the real line such that $X(n + 1) = F_p(X(n))$, where ‘transition probabilities’ are a reflection of the game rules: each realization of the game will correspond to a choice of the initial condition x_0 for its deterministic version F_p . Let us start from game \mathcal{A} : the dynamical realization is easily accomplished once we define F_p on the unit interval as follows:

$$F_{p\mathcal{A}}(x) = \begin{cases} \frac{1}{p}x + 1 & x \in [0, p) \\ \frac{1}{1-p}x - \frac{1}{1-p} & x \in [p, 1) \end{cases} \quad (1)$$

and then extend (1) on the real line by translation symmetry

$$F_{p\mathcal{A}}(x + n) = F_p(x) + n \quad n \in \mathbb{Z} \quad (2)$$

(see figure 1). The left branches of the map correspond to a winning event (capital is increased by one unit, strictly speaking capital corresponds to the integer part of the dynamical variable here) while right branches account for losing events. In the theory we will employ later on together with the map on the real line we also need to consider a corresponding torus map $\hat{F}_p(\vartheta)$ on the circle, that is simply defined as (see figure 2)

$$\hat{F}_{p\mathcal{A}}(\vartheta) = F_p(\vartheta)_{\text{mod } 1}. \quad (3)$$

The construction of a dynamical mapping corresponding to successive playing at \mathcal{B} game is slightly more complicated, as the natural unit is not a single cell, but a group of three cells, due to the mod 3 condition: once we take it into account we may define in this case

$$F_{p\mathcal{B}}(x) = \begin{cases} \frac{1}{p_1}x + 1 & x \in [0, p_1) \\ \frac{1}{1-p_1}x - \frac{1}{1-p_1} & x \in [p_1, 1) \\ \frac{1}{p_2}x - \frac{1}{p_2} + 2 & x \in [1, 1 + p_2) \\ \frac{1}{1-p_2}x - \frac{2}{1-p_2} + 1 & x \in [1 + p_2, 2) \\ \frac{1}{p_2}x - \frac{2}{p_2} + 3 & x \in [2, 2 + p_2) \\ \frac{1}{1-p_2}x - \frac{3}{1-p_2} + 2 & x \in [2 + p_2, 3). \end{cases} \quad (4)$$

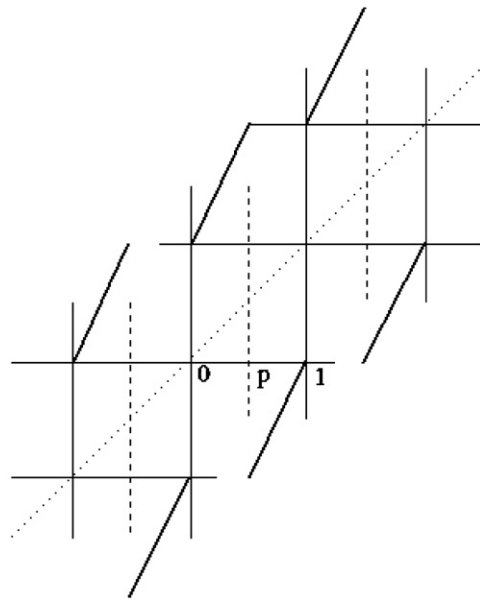


Figure 1. The map corresponding to game \mathcal{A} .

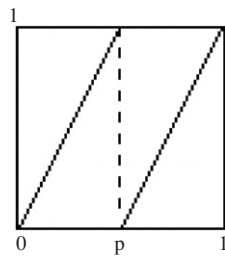


Figure 2. The torus map corresponding to game \mathcal{A} .

Figures 3 and 4 show the corresponding map on the real line and on the (mod 3 torus), respectively. Now we are interested in a random combination of the two games: we call γ the probability that at each step game \mathcal{A} is played ($(1 - \gamma)$ will correspondingly be the probability of playing game \mathcal{B}): though a treatment involving composition of the individual games' transfer operators is possible [5], the simplest way of constructing the relevant dynamical map is to consider combined rates of winning and losing, and then designing the corresponding map. We define

$$q_1 = \gamma p + (1 - \gamma)p_1 \tag{5}$$

and

$$q_2 = \gamma p + (1 - \gamma)p_2. \tag{6}$$

These are the rates of winning if the capital is/is not equal to zero (mod 3): the corresponding dynamical map is then very similar to (4) and precisely

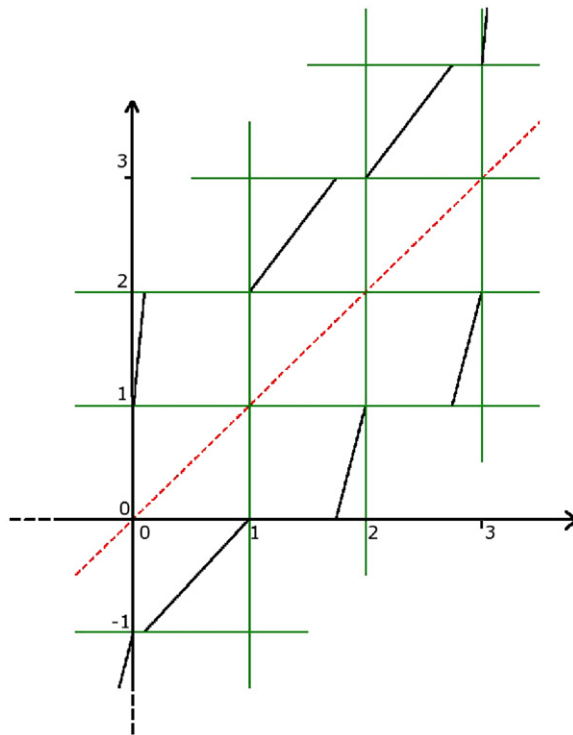


Figure 3. The map corresponding to game \mathcal{B} with $p_1 = 1/10 - \epsilon$, $p_2 = 3/4 - \epsilon$ and $\epsilon = 0.005$.

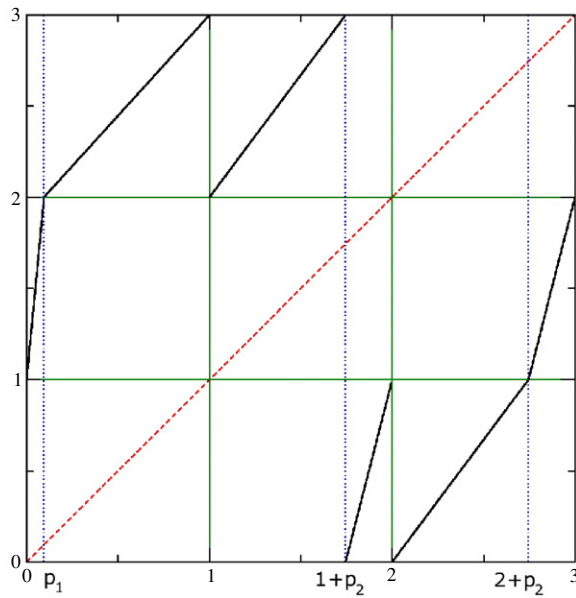


Figure 4. The torus map corresponding to game \mathcal{B} with $p_1 = 1/10 - \epsilon$, $p_2 = 3/4 - \epsilon$ and $\epsilon = 0.005$.

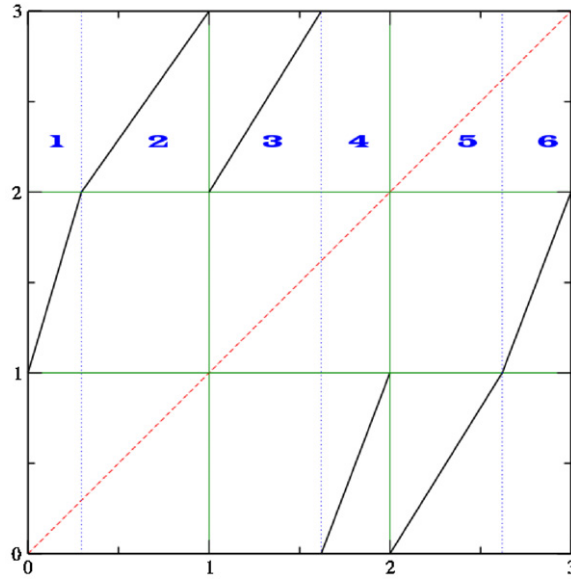


Figure 5. The torus map corresponding to the random composition of games \mathcal{A} and \mathcal{B} with $\gamma = 1/2$.

$$F_{P_{\mathcal{A} \star \mathcal{B}}}(x) = \begin{cases} \frac{1}{q_1}x + 1 & x \in [0, q_1) \\ \frac{1}{1-q_1}x - \frac{1}{1-q_1} & x \in [q_1, 1) \\ \frac{1}{q_2}x - \frac{1}{q_2} + 2 & x \in [1, 1 + q_2) \\ \frac{1}{1-q_2}x - \frac{2}{1-q_2} + 1 & x \in [1 + q_2, 2) \\ \frac{1}{q_2}x - \frac{2}{q_2} + 3 & x \in [2, 2 + q_2) \\ \frac{1}{1-q_2}x - \frac{3}{1-q_2} + 2 & x \in [2 + q_2, 3). \end{cases} \quad (7)$$

The (torus) map is shown in figure 5: the labels $\eta \in \{1, 2, 3, 4, 5, 6\}$ indicated on top of the figure are symbols defining a partition of the unit interval according to the support of the different branches of the map (cf (7)). It is important to remark that in each subinterval η both the slope of the map and the capital gain σ_η are constant: in particular $\sigma_1 = \sigma_3 = \sigma_5 = +1$ (winning intervals) and $\sigma_2 = \sigma_4 = \sigma_6 = -1$ (losing intervals). The slopes (which account for orbit instability) of the different branches are

$$\Lambda_3 = \Lambda_5 = q_2^{-1} \quad \Lambda_4 = \Lambda_6 = (1 - q_2)^{-1} \quad \Lambda_1 = q_1^{-1} \quad \Lambda_2 = (1 - q_1)^{-1}. \quad (8)$$

The asymptotic properties of the combined game in this dynamical context correspond to transport features: we are particularly interested in evaluating the net-directed velocity v

$$\Sigma_1(n) = \langle X_n - X_0 \rangle_0 = v \cdot n \quad (9)$$

and the diffusion coefficient D

$$\Sigma_2(n) = \langle (X_n - X_0)^2 \rangle_0 - v^2 n^2 = 2D \cdot n, \quad (10)$$

where $\langle \cdot \cdot \rangle_0$ denotes an average over a set of initial conditions (for instance uniform distribution on the cell at the origin).

3. Periodic orbit theory

A suitable technique to compute exponents like v and D is via *cycle expansions* [3, 6]: it automatically encompasses universality features, being invariant under topological conjugacies and, while allowing us to get analytic results in the present context, it may be applied—as a genuine perturbative scheme—to possible generalizations (for instance, if we consider maps where piecewise linearity is lost). Such a technique has been applied to other systems exhibiting chaotic transport [7], and also generalized to yield anomalous moments' exponents when intermittency appears [8]. We very briefly recall how v and D are computed: a pedagogical introduction is contained in [9]. The asymptotic behaviour of moments is determined through the generating function

$$G_n(\beta) = \langle e^{\beta(X_n - X_0)} \rangle \quad (11)$$

as

$$\langle (X_n - X_0)^q \rangle = \left(\frac{\partial^q}{\partial \beta^q} G_n(\beta) \right) \Big|_{\beta=0}. \quad (12)$$

In this way one has to characterize the asymptotic behaviour of the generating function: as in statistical mechanics of lattice systems a (generalized) transfer operator \mathcal{L}_β may be introduced, such that

$$G_n(\beta) = \int dx [\mathcal{L}_\beta^n \rho_{\text{in}}](x), \quad (13)$$

where ρ_{in} is the density of initial conditions: thus the leading eigenvalue $\lambda(\beta)$ of the transfer operator dominates the asymptotic behaviour of the generating function

$$G_n(\beta) \sim \lambda(\beta)^n, \quad (14)$$

while the expression for the transfer operator is as follows:

$$[\mathcal{L}_\beta \phi](x) = \int dy e^{\beta(F_P(y) - y)} \delta(F_P(y) - x) \phi(y). \quad (15)$$

A convenient way to compute the leading eigenvalue of \mathcal{L}_β is provided by the *dynamical zeta function* [3, 6] which is expressed as an infinite product over prime periodic orbits of the torus map \hat{F} :

$$\zeta_{(0)\beta}^{-1}(z) = \prod_{\{p\}} \left(1 - \frac{z^{n_p} e^{\beta \sigma_p}}{|\Lambda_p|} \right). \quad (16)$$

Each orbit carries a weight determined by prime period n_p , instability $\Lambda_p = \prod_{i=0}^{n_p-1} \hat{F}'_P(\hat{F}_P^i(x_p))$ and the capital gain σ_p , that is the integer factor that gives the capital variation per cycle once the orbit is unfolded on the real line: if the orbit has symbol sequence $\epsilon_1, \dots, \epsilon_{n_p}$ according to the partition defined earlier, then

$$\sigma_p = \sum_{k=1}^{n_p} \sigma_{\epsilon_k}. \quad (17)$$

The way dynamical zeta functions enter the game is that their smallest zero coincides with the inverse of the leading eigenvalue of the transfer operator [3]: though this might look as a cumbersome way to attack the problem of averages computations, it turns out that if the symbolic dynamics of the system is under control (as in the present example, as we will show later) dynamical zeta functions may provide exact results (as in the Parrondo case), or, in more general examples, they yield a scheme to compute averages in a rapidly converging

perturbative scheme [6, 3]. We call $z(\beta)$ the smallest zero of the dynamical zeta function: by expanding (11, 14) around $\beta = 0$, we get

$$\langle e^{\beta(X_n - X_0)} \rangle \sim \left\langle 1 + \beta(X_n - X_0) + \frac{\beta^2}{2}(X_n - X_0)^2 + \dots \right\rangle$$

$$\lambda(\beta)^n \sim 1 + \beta n \lambda'(0) + \frac{\beta^2}{2} [n(n-1)\lambda'(0)^2 + n\lambda''(0)] + \dots$$
(18)

where we have taken into account that $\lambda(0) = z(0)^{-1} = 1$, as the generalized transfer operator for $\beta = 0$ coincides with the Perron–Frobenius operator whose leading eigenvalue (corresponding to the invariant measure) is $\lambda = 1$. This easily yields v and D in terms of zeta functions [7] (note that all cases dealt with in former papers, however, consider systems where symmetry yields $v = 0$)

$$v = \frac{d\langle X_n - X_0 \rangle}{dn} = \lambda'(0) = - \left(- \frac{\partial_\beta \zeta_{(0)\beta}^{-1}}{\partial_z \zeta_{(0)\beta}^{-1}} \right) \Big|_{\beta=0, z=1}$$
(19)

For the diffusion constant, we get

$$D = \frac{1}{2}(\lambda''(0) - \lambda'(0)^2),$$
(20)

where the first derivative is given by (19), while

$$\lambda''(0) = 2 \left(- \frac{\partial_\beta \zeta_{(0)\beta}^{-1}}{\partial_z \zeta_{(0)\beta}^{-1}} \right)^2 \Big|_{z=1, \beta=0} + \left(\frac{(\partial_z \zeta_{(0)\beta}^{-1})^2 \partial_{\beta\beta} \zeta_{(0)\beta}^{-1} + (\partial_\beta \zeta_{(0)\beta}^{-1})^2 \partial_{zz} \zeta_{(0)\beta}^{-1} - 2\partial_\beta \zeta_{(0)\beta}^{-1} \partial_z \zeta_{(0)\beta}^{-1} \partial_{z\beta} \zeta_{(0)\beta}^{-1}}{(\partial_z \zeta_{(0)\beta}^{-1})^3} \right) \Big|_{z=1, \beta=0}$$
(21)

4. Parrondo transport from zeta functions

In order to use formulae like (19, 21) for the deterministic version of Parrondo games, we have to provide an expression for the zeta function. This is done once we set up the symbolic rules for dynamics: by considering the torus map $\hat{F}_{P,A*B}$ (see figure 5), the only allowed symbolic transitions are the following:

$$\begin{array}{cccc} \dots 13 \dots & \dots 14 \dots & \dots 25 \dots & \dots 26 \dots \\ \dots 35 \dots & \dots 36 \dots & \dots 41 \dots & \dots 42 \dots \\ \dots 51 \dots & \dots 52 \dots & \dots 63 \dots & \dots 64 \dots \end{array}$$
(22)

thus admissible symbolic sequences are generated by the Markov graph of figure 6. As the weights we attach to cycles depend only on how many times different symbols appear in the cycle code, our problem is essentially topological and the zeta function is a polynomial, which we can easily write once we have the full list of non-intersecting loops of the Markov graph of figure 6. These are

$$\overline{14} \overline{25} \overline{36} \overline{135} \overline{264} \overline{1364} \overline{1425} \overline{2635} \overline{135} \overline{264} \overline{136} \overline{425} \overline{142} \overline{635}$$
(23)

Then [10, 11]

$$\zeta_{(0)\beta}^{-1} = \sum_{k=0}^f \sum_{\pi} (-1)^k t_{p_1} \dots t_{p_k},$$
(24)

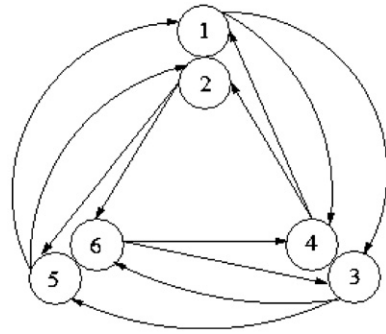


Figure 6. The Markov graph generating symbol sequences for the map $\hat{F}_{P,A \times B}$.

where all possible combinations π of non-intersecting loops $p_1 \cdots p_k$ are considered, f is the maximum number of non-intersecting loops that we may put on the graph and

$$t_p = \frac{z^{n_p} e^{\beta \sigma_p}}{\Lambda_p}. \tag{25}$$

Once we take into account cancellations (for instance the cycle $\overline{142635}$ is completely shadowed by the product of $\overline{14}$ and $\overline{2635}$ cycles), the generalized zeta function is written as

$$\begin{aligned} \zeta_{(0)\beta}^{-1}(z) &= 1 - z^2 \left(\frac{e^{\beta \sigma_{14}}}{\Lambda_{14}} + \frac{e^{\beta \sigma_{25}}}{\Lambda_{25}} + \frac{e^{\beta \sigma_{36}}}{\Lambda_{36}} \right) - z^3 \left(\frac{e^{\beta \sigma_{135}}}{\Lambda_{135}} + \frac{e^{\beta \sigma_{264}}}{\Lambda_{264}} \right) \\ &= 1 - z^2 (q_1(1 - q_2) + q_2(1 - q_1) + q_2(1 - q_2)) + \\ &\quad - z^3 (e^{3\beta} q_1 q_2^2 + e^{-3\beta} (1 - q_1)(1 - q_2)^2), \end{aligned} \tag{26}$$

where we have taken into account how instabilities (8) are expressed in terms of transition probabilities (5, 6) and used the capital gains $\sigma_{14} = \sigma_{25} = \sigma_{36} = 0$, $\sigma_{135} = 3$ and $\sigma_{264} = -3$. Now we take the original Parrondo values

$$p = \frac{1}{2} - \epsilon \quad p_1 = \frac{1}{10} - \epsilon \quad p_2 = \frac{3}{4} - \epsilon \tag{27}$$

and take $\gamma = 1/2$: once we insert (26) into (19), we may verify Parrondo paradox, namely how unfair games (for small positive ϵ) lead to capital gain: see figure 7, and in the same way we may look at the behaviour of the diffusion coefficient (see figure 8). In the same fashion we may check how transport exponents depend on the parameter γ once the bias ϵ is fixed (see the current behaviour in figure 9).

It turns out that by using the explicit form of the zeta function, we can actually derive analytical expressions for such quantities: for instance, the current v as a function of ϵ for $\gamma = 1/2$ reads (in agreement with [4])

$$v_{1/2}(\epsilon) = \frac{6(3 - 229\epsilon + 16\epsilon^2 - 320\epsilon^3)}{709 - 32\epsilon + 960\epsilon^2}, \tag{28}$$

or, expressed as a first-order expansion in ϵ ,

$$v_{1/2}(\epsilon) = \frac{18}{709} - \frac{973\,590}{502\,681}\epsilon + O(\epsilon)^2 \tag{29}$$

from which the small ϵ paradoxical behaviour is explicitly seen. More generally, we can express the current v as a function of both ϵ and γ as

$$v_\gamma(\epsilon) = \frac{6(-80\epsilon^3 + 8(1 - \gamma)\epsilon^2 - (11(2 - \gamma)\gamma + 49)\epsilon + 2(1 - \gamma)(2 - \gamma)\gamma)}{240\epsilon^2 - 16(1 - \gamma)\epsilon + 11(2 - \gamma)\gamma + 169}. \tag{30}$$

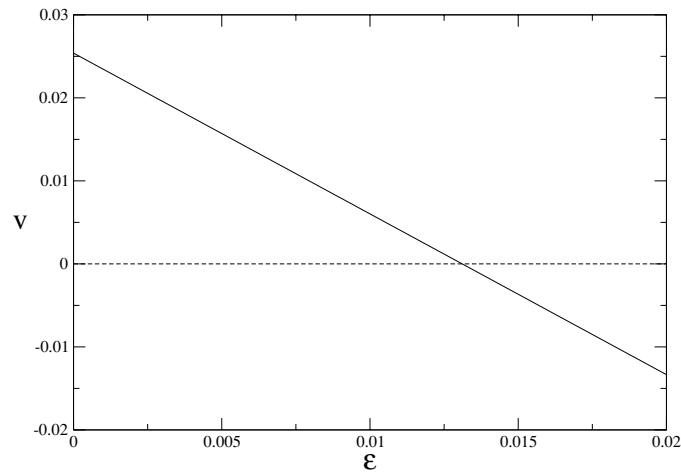


Figure 7. The current v as a function of ‘unfairness’ parameter ϵ for small positive ϵ ($\gamma = 1/2$). Note the current inversion at $\epsilon \approx 0.0131$.

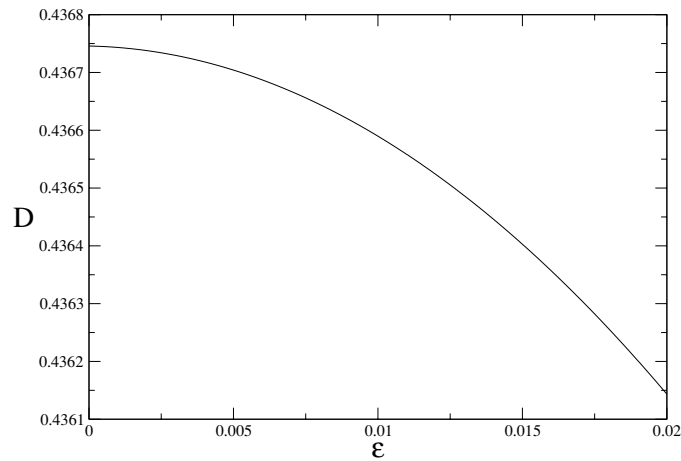


Figure 8. The diffusion coefficient D as a function of ‘unfairness’ parameter ϵ ($\gamma = 1/2$).

Analytic expression may be obtained also for the diffusion constant D , for instance

$$D_{1/2}(\epsilon) = -(9(4\epsilon(\epsilon(64\epsilon(\epsilon(64\epsilon(5\epsilon(320\epsilon(15\epsilon - 2) + 9243) - 4487) + 1458\ 885) + 69\ 761) - 6333\ 811) + 1191\ 650) - 34\ 590\ 345))/(2(32\epsilon(30\epsilon - 1) + 709)^3). \quad (31)$$

Generalizing to $M > 3$, the same qualitative behaviour would be obtained, after adjusting the probability values. Differently, for $M = 2$, the paradox is not possible: the randomized game maintains the same nature (loosing, fair or winning) as the native ones. The zeta function in this case is

$$\zeta_{(0)\beta}^{-1}(z) = 1 - z^2(q_1(1 - q_2) + q_2(1 - q_1)) - z^2(e^{2\beta}q_1q_2 + e^{-2\beta}(1 - q_1)(1 - q_2)), \quad (32)$$

which leads to the following equation for the current v :

$$v(q_1, q_2) = \frac{q_1 + q_2 - 1}{2}. \quad (33)$$

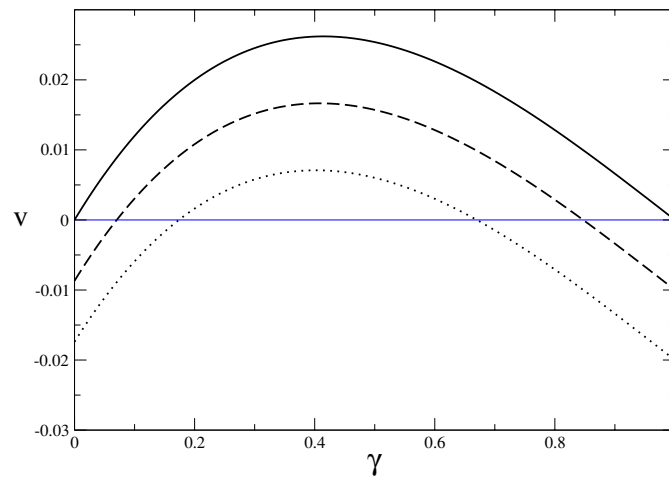


Figure 9. The current v as a function of γ for $\epsilon = 0$ (full line), $\epsilon = 0.005$ (dashed line) and $\epsilon = 0.01$ (dotted line). Maxima are attained at $\gamma = 0.414\,588$, $\gamma = 0.408\,161$ and $\gamma = 0.401\,643$, respectively.

In order to have the paradox, the following inequalities need to be simultaneously satisfied:

$$p < \frac{1}{2}, \quad p_1 + p_2 < 1, \quad q_1 + q_2 > 1, \quad (34)$$

which is impossible (the same result can be obtained via a Markov chains analysis).

5. Conclusions

We have constructed a one-dimensional mapping providing a deterministic version of Parrondo games: once the symbolic dynamics is coded, periodic orbit theory offers a way to get analytic estimates of all the relevant transport exponents. While in this paradigmatic example results may be obtained via probabilistic techniques [4, 12] we remark two things: once the structure of the relevant zeta function is explicitly derived, all statistical averages may be computed in a similar way in the present framework: moreover, our work may be considered as a first step towards the periodic orbit analysis of ‘nonlinear’ Parrondo games, where the map ceases to be piecewise linear: in particular, we plan to investigate sticking effects in this context, by considering intermittent Parrondo maps.

Acknowledgment

This work was partially supported by the PRIN 2003 Project *Order and Chaos in Nonlinear Extended Systems*.

References

- [1] Reimann P 2002 *Phys. Rep.* **361** 57
- [2] Harmer G P and Abbott D 1999 *Stat. Sci.* **14** 206
Harmer G P and Abbott D 2002 *Fluctuation Noise Lett.* **2** R71
- [3] Cvitanović P, Artuso R, Mainieri R, Tanner G and Vattay G 2005 *Chaos: Classical and Quantum* (Copenhagen: Niels Bohr Institute) (ChaosBook.org)
- [4] Harmer G P, Abbott D, Taylor P G and Parrondo J M R 2001 *Chaos* **11** 705

-
- [5] Dabaghian Y 2001 *Phys. Rev. E* **63** 046209
 - [6] Artuso R, Aurell E and Cvitanović P 1990 *Nonlinearity* **3** 326
Artuso R, Aurell E and Cvitanović P 1990 *Nonlinearity* **3** 361
 - [7] Artuso R 1991 *Phys. Lett. B* **160** 528
Cvitanović P, Gaspard P and Schreiber T 1992 *Chaos* **2** 85
Artuso R and Strepparava R 1997 *Phys. Lett. A* **236** 469
 - [8] Artuso R and Cristadoro G 2003 *Phys. Rev. Lett.* **90** 244101
Artuso R and Cristadoro G 2004 *J. Phys.: Condens. Matter A* **37** 85
 - [9] Artuso R 2003 *Lecture Notes in Physics* vol 618 p 145
 - [10] Cvitanović P 2005 *Counting for pedestrians in Chaos: Classical and Quantum* (Copenhagen: Niels Bohr Institute) (ChaosBook.org)
 - [11] Cvektović D M, Doob M and Sachs H 1980 *Spectra of Graphs* (New York: Academic)
 - [12] Artuso R, Cavallasca L and Cristadoro G 2005 (unpublished) v and D may be computed in the framework of periodic hopping models as in Derrida B and Pomeau Y 1982 *Phys. Rev. Lett.* **48** 627
Derrida B 1983 *J. Stat. Phys.* **31** 433